PHYSICAL REVIEW A VOLUME 44, NUMBER 7 1 OCTOBER 1991

Quadrupole moments as measures of electron correlation in two-electron atoms

Sandra C. Ceraulo and R. Stephen Berry
Department of Chemistry and The James Franck Institute, The University of Chicago, Chicago, Illinois 60637

(Received 11 February 1991)

We have calculated quadrupole moments, Q_{zz}, of helium in several of its doubly excited states and in two of its singly excited Rydberg states, and of the alkaline-earth atoms Be, Mg, Ca, Sr, and Ba in their ground and low-lying excited states. The calculations use well-converged, frozen-core configuration-interaction (CI) wave functions and, for interpretive purposes, Hartree-Fock (HF) atomic wave functions and single-term, optimized, molecular rotor-vibrator (RV) wave functions. The quadrupole moments calculated using RV wave functions serve as a test of the validity of the correlated, moleculelike model, which has been used to describe the effects of electron correlation in these two-electron and pseudo-two-electron atoms. Likewise, the quadrupole moments calculated with HF wave functions test the validity of the independent-particle model. In addition to their predictive use and their application to testing simple models, the quadrupole moments calculated with CI wave functions reveal previously unavailable information about the electronic structure of these atoms. Experimental methods by which these quadrupole moments might be measured are also discussed. The quadrupole moments computed from CI wave functions are presented as predictions; measurements of Q_{zz} have been made for only two singly excited Rydberg states of He, and a value of Q_{zz} has been computed previously for only one of the states reported here. We present these results in the hope of stimulating others to measure some of these quadrupole moments.

PACS number(s): 31.20.Tz, 31.90.+s, 32.90.+a

I. INTRODUCTION

Since the observation of highly mixed ${}^1P^o$ channels in doubly excited helium (He**) by Madden and Codling in 1963 [1,2], there has been a great deal of interest in electron correlation in two-electron atoms. Much of this interest has focused on theoretical models and physical interpretations of that correlation; some attention has been paid to observable manifestations but perhaps not as much as modern experimental methods permit. Here, we discuss one property, the atomic quadrupole moment, which can be treated as both an observable and as a criterion for the relative validity of competitive models. We present values of the quadrupole moments of a number of states of helium and of the alkaline-earth elements calculated from three kinds of wave functions: a set believed to be well converged and therefore reliable enough to guide or even predict results of experiments; a set based on the Hartree-Fock wave functions appropriate to an independent-particle model of the valence electrons; and a set of highly correlated, moleculelike wave function appropriate to a collective model of the valence electrons. The comparisons of values obtained from the extreme models with the values from the well-converged functions serve as tentative tests of the relative validity of those models as interpretive tools. The values based on the well-converged functions will, we hope, stimulate experiments to measure atomic quadrupole moments whose comparisons with all three kinds of computed values will test the "accurate" values and put the validating tests of the conceptual models on a firm footing.

Two approaches, the adiabatic hyperspherical model [3] and the molecular model [4,5], have been used to represent the dynamics of these highly correlated two-electron and pseudo-two-electron systems. Here, we focus on the molecular model that has recently been reviewed by Berry [6] and by Berry and Krause [7]. Attention first centered on the doubly excited states of helium [8–10] but was later extended to the more experimentally tractable ground and low-lying excited states of alkaline-earth-metal atoms [11,12] and the alkali-metal negative ions [13]. This model, while based on well-converged variational wave functions, interprets the two-electron, three-body, *e*-nucleus-*e* system as a "linear triatomic molecule" which undergoes rotational and vibrational motion and that can be described by the rotational and vibrational quantum numbers used to characterize molecules. This molecular interpretation was first suggested by Kellman and Herrick [4,5] when they showed that the phenomenological classification they found that best reproduces the observed the energy-level spacings in He** can be made isomorphic to that of a linear triatomic molecule.

Evidence in support of the molecular model has come in several forms. One consists of the spatial probability distributions calculated in the internal *e*-core-*e* coordinate system from well-converged configuration-interaction (CI) wave functions derived using frozen-core pseudopotentials [12]. Graphic representations based on reduced probability distributions revealed that two-electron, three-body systems have "shapes," i.e., spatial distributions of conditional probability density, similar to those of a floppy, linear triatomic molecule in its characteristic rotational and vibrational modes. This earlier evidence was chiefly qualitative; the evaluation of the molecular model was then put on a quantitative footing by the calculation of the overlaps between the CI wave functions and simple, optimized molecular rotor-vibrator (RV) wave functions developed explicitly for the two-electron atoms [14]. The squares of these overlaps were generally greater than 90% and gave a measure of the varying degree of collective, molecular motion in states of various symmetries of the different two-electron atoms. For example, overlaps were generally very high for the e^1S^e "ground rotor" state and the $^3P^e$ "bending" state, but tended to be a little lower for $^1S^e$ and $^3S^e$ intershell "symmetric and antisymmetric stretching" states and for the $^1P^o$ "bending" state. More recently, oscillator strengths for helium and the alkaline-earth-metal elements were calculated with the CI wave functions developed earlier [15]. These were found to be in good agreement with experimental oscillator strengths, and thus confirmed that the pseudopotential-based CI wave functions were of reliable accuracy. Furthermore, for the purpose of comparison, oscillator strengths were also calculated using the single-term molecular RV wave functions developed for the two-electron atoms to test the validity of a collective model. These were compared with calculated values based on all-electron Hartree-Fock (HF) wave functions, which measured the validity of the independent-particle model, as well as with values on the CI wave functions. For most but by no means all of the transitions, the RV oscillator strengths were in better agreement with accurately calculated oscillator strengths reported in the literature than were the HF oscillator strengths.

In the present work, we calculate electric quadrupole moments for doubly excited helium and the alkaline-earth elements in their ground and low-lying excited states. This calculation is analogous to the oscillator strength calculation described above except that here we compare our CI quadrupole moments to those calculated with frozen-core, pseudopotential-based Hartree-Fock wave functions while the CI oscillator strengths were compared to those calculated with all-electron Hartree-Fock wave functions. The quadrupole moment of a two-electron system may well be expected to be a more sensitive measure of the effects of correlation than the predominantly one-electron property of oscillator strength. Quadrupole moments have been used for many years as probes of nuclear "shapes" [16] and have been used to some extent to study spatial distributions of charge in atoms and molecules, as described below.

Once again an observable that can be written as a spherical tensor is calculated using well-converged CI wave functions and, for the purpose of comparison, both molecular RV wave functions and atomic HF wave functions. Except in the case of the $2s2p\ ^3P_2^o$ and $^3P_1^o$ states of beryllium [17], there seem to be no previously computed quadrupole moments for two-electron atoms calculated using HF wave functions, and thus, we present our own here. Once again, can compare an *observable* accurately calculated with CI wave functions, to that calculated using two zeroth-order models, the independent-particle model represented by HF quadrupole moments and the molecular, collective model represented by RV quadrupole moments.

To estimate the accuracy of the CI quadrupole moments, we have developed CI wave functions for He $1s4p\ 4\,^3P$ and $1s5p\ 5\,^3P$ states and used them to calculate quadrupole moments for these states. The large difference in the two electrons' principal quantum numbers in these singly excited states leads to the expectation that they should not be highly correlated, indeed, they should be exemplars of independent particle motion. However, these are, to our knowledge, the only excited atomic states for which quadrupole moments have been measured [18,19], and they thus allow us to compare two of our CI quadrupole moments, which are calculated in the same manner as all the others, with experimental results. Furthermore, to test the accuracy of the newly derived CI wave functions for these singly excited helium states, we have calculated oscillator strengths for the He $1s2s\ ^3S^e \rightarrow 1s4p\ ^3P^o$ and $1s2s\ ^3S^e \rightarrow 1s5p\ ^3P^o$ transitions. As Hunter and Berry did with oscillator strengths for transitions between highly correlated states of two-electron atoms, we compare our CI oscillator strengths for these transitions to the accurately calculated oscillator strengths for them that are available in the literature [20]. Thus, we are able to obtain an independent estimate of the reliability of these two new CI wave functions which, in this case, represent predominantly independent particle motion.

Although we are not aware of any measurements of the electric quadrupole moments of the highly correlated states of helium and the alkaline-earth atoms, direct measurements of electric quadrupole moments of similar systems have been made for some time. The first direct measurement of a molecular, electric quadrupole moment was reported in 1964 when the quadrupole moment of CO_2 was measured by Buckingham and Disch using optical birefringence [21]. Direct measurements of atomic electric quadrupole moments began in 1967 when Angel, Sandars, and Woodgate measured the quadrupole moment of the $^2P_{3/2}$ ground state of aluminum using atomic beam magnetic resonance [22]. Miller and Freund made the first direct measurement of the electric quadrupole moment of an atom in an *excited* state in 1971 when they determined the quadrupole moment of the $1s4p\ 4\,^3P$ state of helium using the diamagnetic Zeeman effect [18,19] as earlier mentioned. The latter two experimental methods, which were used on atoms, appear to be the most promising for measurement of the quadrupole moments calculated here and will be discussed further in Sec. III of this paper.

In addition to serving as an observable that can test the validity of the molecular model, the quadrupole moments calculated using CI wave functions reveal previously unavailable quantitative and qualitative information about the electronic structure of the atoms. The quadrupole moment is a second rank tensor most commonly defined by the equation

$$Q_{jk}=\tfrac{1}{2}\sum_i q_i(3j_ik_i-r_i^2\delta_{jk}) \quad (j,k=x,y,z)\ , \tag{1}$$

where the sum is over all the charges of the system and the indices j and k denote the nine Cartesian components of the tensor. [The quadrupole moment is sometimes defined by a slightly different equation that differs from Eq. (1) by a factor of 2 or -2.] If the system of charges is cylindrically symmetric, as is the case in a two-electron atom, all off-diagonal components of the quadrupole moment tensor vanish in the principal-axis representation. When combined with the fact that the quadrupole moment matrix is traceless, this means that there is only one independent component of the quadrupole moment tensor in a cylindrically symmetric system. If the axis of cylindrical symmetry is taken as the z axis as is the usual convention, then the diagonal components of the quadrupole moment tensor are related: $Q_{zz}=-2Q_{xx}=-2Q_{yy}$. In such cases, Q_{zz} is usually referred to as *the* quadrupole moment. Adaptation of Eq. (1) to a cylindrically symmetric quantum mechanical two-electron atom yields

$$\langle Q_{zz}\rangle=-\tfrac{1}{2}e\sum_{i=1}^{2}\langle 3z_i^2-r_i^2\rangle \ . \tag{2}$$

Equation (2) reveals that a negative atomic quadrupole moment indicates a prolate electronic charge distribution, and a positive quadrupole moment indicates an oblate electronic charge distribution. Similarly, Eq. (2) shows that the quadrupole moment of a spherically symmetric charge distribution must vanish.

Atomic quadrupole moments are characterized by the total angular momentum J and by its projection on the space-fixed z axis which is represented by the magnetic quantum number M_J, i.e., the quadrupole moment is usually [22] given by

$$\langle Q_{zz}\rangle=-\tfrac{1}{2}e\sum_{i=1}^{2}\langle J,M_J=J|3z_i^2-r_i^2|J,M_J=J\rangle \ . \tag{3}$$

The *mean* quadrupole moment for any given state, that is the sum of the quadrupole moments of states with different magnetic quantum numbers divided by $2J+1$, must vanish. This is because the spherical average of any tensor for $J>0$ must be zero, corresponding to an average spherically symmetric charge distribution. In addition, well-known symmetry rules dictate that only states with $J\geq 1$ can have a nonvanishing quadrupole moment. The *nsn* $^1S^e$ ground "rotor" states of the alkaline earths and the $ns(n+1)s$ $^1S^e$ excited "symmetric stretch" states that have $J=0$ therefore must have zero quadrupole moments.

Two other constraints, based on the space quantization inherent in the atom, relate the quadrupole moments of the M_J states with the same total angular momentum J of a given atom to each other. The first such constraint is that the quadrupole moments must be symmetric about $M_J=0$ since it is the absolute value of the magnetic quantum number that dictates the "shape" of the charge distribution. The second such constraint on quadrupole moments in the laboratory frame is that values for different M_J states must be in the same ratio as the corresponding values of $3\cos^2\theta-1$ where θ is the space-quantized angle between the space-fixed z axis and the direction of the total angular momentum. For a state in which both J and M_J are known, it is elementary to evaluate this quantity. For example, for two states of an atom in which $J=2$, the quadrupole moments for $M_J=2$ and $M_J=1$ are related:

$$\frac{Q_{J=2,M_J=2}}{Q_{J=2,M_J=1}}=\frac{3[M_J/\sqrt{J(J+1)}]^2-1}{3[M_J/\sqrt{J(J+1)}]^2-1}=\frac{3[2/\sqrt{2(3)}]^2-1}{3[1/\sqrt{2(3)}]^2-1}=-2 \ . \tag{4}$$

The space-quantized angle above is *not* the same as the expectation value of the polar angles that are arguments of the spherical harmonics and that are discussed later in this paper, for example in Eq. (17). The expectation values of the cosines of the polar angles of any two different M_J states are in the same ratio as the fixed angles between the space-fixed z axis and the directions of the total angular momenta for the same M_J states. The above three constraints taken together yield the interesting result that for any atomic state with $J\leq 2$, within any J state the quadrupole moments of all the M_J states may be written in terms of the quadrupole moment of any single M_J state.

The organization of this paper is as follows. In Sec. II we discuss the forms of the wave functions employed here. In Sec. III we present the calculated quadrupole moments together with the squares of the overlaps between the three sets of wave functions used, and then we discuss the significance of these results as well as the most promising experimental methods that might be used to verify them.

II. WAVE FUNCTIONS FOR TWO-ELECTRON ATOMS

A. Configuration-interaction (CI) wave functions

We use the CI wave functions of Ezra and Berry [9] for helium and those of Krause and Berry [12] for alkaline-earth-metal atoms. The alkaline-earth wave functions were constructed by using the pseudopotentials of Bachelet, Hamann, and Schlüter [23] for the electronic cores which were assumed to be non-polarizable. The CI wave functions are of the form

$$\Psi_{\mathrm{CI}}=\mathcal{A}\sum_{l_1,n_1,l_2,n_2}C_{l_1n_1l_2n_2}\phi_{n_1l_1}(r_1)\phi_{n_2l_2}(r_2)\mathcal{Y}_{l_1l_2}^{LM}(\hat{\mathbf{r}}_1,\hat{\mathbf{r}}_2) \ , \tag{5}$$

where the radial basis functions are Sturmian functions of the form

$$\phi_{n,l}(r)=\mathcal{N}r^{n-1}e^{-\xi r} \ , \quad n>l \tag{6}$$

and the angular basis functions are coupled spherical harmonics,

$$\mathcal{Y}_{l_1l_2}^{LM}(\hat{\mathbf{r}}_1,\hat{\mathbf{r}}_2)=\sum_{m_1,m_2}\langle l_1m_1l_2m_2|LM\rangle \times Y_{l_1m_1}(\theta_1,\phi_1)Y_{l_2m_2}(\theta_2,\phi_2) \ . \tag{7}$$

Here, $\mathcal{A}$ is an antisymmetrization operator, C is an expansion coefficient, and $\mathcal{N}$ is a normalization constant. The quantum numbers have their usual meanings.

B. Unrestricted Hartree-Fock (UHF) wave functions

The unrestricted Hartree-Fock wave functions used here were derived by Batka and Berry [24] using unrestricted unrestricted Hartree-Fock open-shell theory. In this theory, electrons are not restricted to being in pairs in closed shells. This method generates less involved spatial equations and tends to give a better variational energy than does the restricted open-shell Hartree-Fock theory. The pseudopotentials of Bachelet, Hamann, and Schlüter, which were used to generate CI wave functions for the alkaline earths, were also used to generate the UHF wave functions. The form of the UHF wave functions is given by

$$\Psi_{\mathrm{UHF}}=\mathcal{A}\sum_{n_1,n_2} C_{n_1n_2}\phi_{n_1l_1}(r_1)\phi_{n_2l_2}(r_2)\mathcal{Y}^{LM}_{l_1l_2}(\hat{\mathbf{r}}_1,\hat{\mathbf{r}}_2)\ . \tag{8}$$

The quantities here are similar to those in Eq. (5) except that the radial basis functions are Slater-type orbitals (STO's) of the form

$$\phi_{n,l}(r)=\frac{(2\zeta/a_0)}{[(2n)!]^{1/2}}r^{n-1}e^{-\zeta r/a_0}\ . \tag{9}$$

The angular functions are again coupled spherical harmonics. An important difference between the CI and UHF wave functions is that the UHF wave functions contain only one angular function.

C. Molecular rotor-vibrator (RV) wave functions

Quadrupole moments are also calculated using Morse local-mode molecular wave functions [14] that were explicitly derived for helium and the alkaline earth atoms. They are the wave functions that were found by Hunter and Berry to maximize the overlap with the atomic CI wave functions. They are of the form

$$\Psi_{\mathrm{RV}}=\mathcal{A}\frac{1}{r_1r_2}R^{\pm}_{nm}(r_1,r_2)G^{k}_{v_2}(\theta_{12})\left[\frac{2J+1}{8\pi^2}\right]^{1/2}\times\mathcal{D}^{J*}_{Mk}(\alpha\beta\gamma)\ , \tag{10}$$

where

$$R^{\pm}_{nm}(r_1,r_2)=\tfrac{1}{2}(2-\delta_{nm})^{1/2}[g_n(r_1)g_m(r_2)\pm g_m(r_1)g_n(r_2)]\ , \tag{11}$$

$$g_n(r)=\mathcal{N}e^{-z/2}z^{b/2}L^{b}_{n}(z)\ , \tag{12}$$

$$z=\kappa e^{-a(r-r_e)}\ , \tag{13}$$

$$b=\kappa-2n-1\ , \tag{14}$$

$$G^{k}_{v_2}(\theta_{12})=\mathcal{N}\rho_2^{|k|}e^{-\rho_2^2/2}L^{|\mathbf{k}|}_{(v_2-|\mathbf{k}|)/2}(\rho_2^2)\ , \tag{15}$$

$$\rho_2=\left[\frac{m_e\omega_2}{2\hbar}\right]^{1/2}(\pi-\theta_{12})r_e\ . \tag{16}$$

Here, v_2 is the number of quanta in the doubly degenerate bending mode, ρ_2 is the corresponding dimensionless normal coordinate, and ω_2 is the corresponding vibrational frequency. The subscripts n and m are the number of vibrational quanta in the two equivalent "bonds." J is the total angular momentum exclusive of spin (equivalent to the atomic L) and M is its projection on the space-fixed z axis; k is the vibrational angular momentum about the body-fixed z' axis. $\mathcal{D}^{J}_{Mk}(\alpha\beta\gamma)$ is a rotation matrix (in the convention of Brink and Satchler [25]) whose arguments are the Euler angles which effect the transformation from the space-fixed frame to the body-fixed frame, m_e is the mass of an electron, and r_e is the equilibrium electron-nucleus separation. $\mathcal{A}$ is an antisymmetrization operator, and $L^{\alpha}_{n}(x)$ is an associated Laguerre polynomial in the convention of Gradshteyn and Ryzhik [26]. The $\mathcal{N}$'s are normalization constants. As explained in Ref. [14], r_e, ω_2, and the Morse parameters κ and a were varied to maximize the overlap with the atomic CI wave functions.

III. RESULTS AND DISCUSSION

The expectation value $\langle z_i^2\rangle$ is given by

$$\langle z_i^2\rangle=\langle JM_J=J|r_i^2\cos^2\theta_i|JM_J=J\rangle\ . \tag{17}$$

For CI and UHF calculations in which the wave functions are written in terms of the electrons' polar and azimuthal angles, the quadrupole moment may be constructed from this and $\langle r^2\rangle$ or the quadrupole moment may be calculated directly. The latter is, of course, computationally more efficient but sacrifices some, however slight, insight into the "geometric" structure of the atom. To calculate the quadrupole moment with the RV wave functions, we wrote the operator first in terms of body-fixed coordinates since the molecular wave functions are written in terms of these and as a spherical tensor operator. Then, in the usual way [27], we summed over all the projections of the spherical tensor to rotate from body-fixed frame to space-fixed frame. Thus,

$$Q^2_{m=0}=\sum_q\mathcal{D}^{2*}_{m=0,q}(\alpha,\beta,\gamma)Q^2_q(r_1,r_2,\theta_{12})\ .$$

Table I lists calculated values for $\langle Q_{zz}\rangle$, $\langle z_1^2\rangle$, and $\langle r_1^2\rangle$ in the space-fixed frame using CI, UHF, and RV wave functions. The squared overlaps between the accurate CI and the UHF wave functions, $S^2_{\mathrm{CI,UHF}}=|\langle\mathrm{CI}|\mathrm{UHF}\rangle|^2$, the squared overlaps between the accurate CI and the RV wave functions, $S^2_{\mathrm{RV,CI}}=|\langle\mathrm{CI}|\mathrm{RV}\rangle|^2$ (taken from Ref. [14]), and the squared overlaps between the RV and UHF wave functions, $S^2_{\mathrm{RV,UHF}}=|\langle\mathrm{RV}|\mathrm{UHF}\rangle|^2$ are also listed. As discussed in Sec. I, the quadrupole moments of all states having $J=0$ vanish in the space-fixed frame.

Figures 1–4 are scatter plots of quadrupole moments for the four P and D series which have nonvanishing quadrupole moments. Note that Ba configurations do not fit the *npnp* description due to mixing with the 6*s*5*d* configuration. In Fig. 1, the quadrupole moments appear to increase, generally, with increasing atomic mass. However this could be serendipitous since no such pattern is apparent in Figs. 2–4.

On the basis of the values in Table I, what can be said

TABLE I. Space-fixed quadrupole moments $\langle Q_{zz}\rangle$, and their components as calculated with CI, UHF, and RV wave functions. All calculations are for $J=J_{\max}$, $M_J=J$ states; see discussion in text regarding quadrupole moments of other states.

State	CI	UHF	RV
He $2s2p\ {}^3P_2^o$			
$\langle Q_{zz}\rangle$	2.622		3.026
$\langle z_1^2\rangle$	3.233		3.308
$\langle r_1^2\rangle$	12.32		12.95
He $2p2p\ {}^1D_2^e$			
$\langle Q_{zz}\rangle$	5.015		3.871
$\langle z_1^2\rangle$	2.498		2.973
$\langle r_1^2\rangle$	12.51		12.79
He $2s2p\ {}^1P_1^o$			
$\langle Q_{zz}\rangle$	0.6929		1.656
$\langle z_1^2\rangle$	4.456		4.275
$\langle r_1^2\rangle$	14.06		14.48
He $2p2p\ {}^3P_2^e$			
$\langle Q_{zz}\rangle$	−2.357		−2.365
$\langle z_1^2\rangle$	4.716		4.732
$\langle r_1^2\rangle$	11.79		11.83
Be $2s2p\ {}^3P_2^o$			
$\langle Q_{zz}\rangle$	2.140	1.833	1.919
$\langle z_1^2\rangle$	2.137	2.168	2.280
$\langle r_1^2\rangle$	8.551	8.336	8.759
Be $2p2p\ {}^1D_2^e$			
$\langle Q_{zz}\rangle$	5.795		4.219
$\langle z_1^2\rangle$	2.458		2.704
$\langle r_1^2\rangle$	13.17		12.33
Be $2s2p\ {}^1P_1^o$			
$\langle Q_{zz}\rangle$	2.783		1.538
$\langle z_1^2\rangle$	3.149		3.231
$\langle r_1^2\rangle$	12.23		11.23
Be $2p2p\ {}^3P_2^e$			
$\langle Q_{zz}\rangle$	−2.073	−2.042	−2.076
$\langle z_1^2\rangle$	4.144	4.084	4.152
$\langle r_1^2\rangle$	10.36	10.21	10.38
Mg $3s3p\ {}^3P_2^o$			
$\langle Q_{zz}\rangle$	3.972		3.212
$\langle z_1^2\rangle$	3.423		3.523
$\langle r_1^2\rangle$	14.24		13.78
Mg $3s3d\ {}^1D_2^e$			
$\langle Q_{zz}\rangle$	14.74		9.194
$\langle z_1^2\rangle$	5.200		4.545
$\langle r_1^2\rangle$	30.34		22.83
Mg $3s3p\ {}^1P_1^o$			
$\langle Q_{zz}\rangle$	5.174		2.199
$\langle z_1^2\rangle$	4.812		5.080
$\langle r_1^2\rangle$	19.61		17.44
Mg $3p3p\ {}^3P_2^e$			
$\langle Q_{zz}\rangle$	−3.622	−3.428	−3.616
$\langle z_1^2\rangle$	8.451	6.856	8.437
$\langle r_1^2\rangle$	18.11	17.14	18.08
Ca $4s4p\ {}^3P_2^o$			
$\langle Q_{zz}\rangle$	6.121	6.630	5.324
$\langle z_1^2\rangle$	5.233	5.210	5.375
$\langle r_1^2\rangle$	21.82	22.26	21.45
Ca $4s3d\ {}^1D_2^e$			
$\langle Q_{zz}\rangle$	1.727		5.676
$\langle z_1^2\rangle$	3.744		2.565
$\langle r_1^2\rangle$	12.96		13.37
Ca $4s4p\ {}^1P_1^o$			
$\langle Q_{zz}\rangle$	4.919	6.630	1.988
$\langle z_1^2\rangle$	6.710	6.003	7.254
$\langle r_1^2\rangle$	25.05	24.64	23.75
Ca $4p4p\ {}^3P_2^e$			
$\langle Q_{zz}\rangle$	−5.215	−5.642	−5.236
$\langle z_1^2\rangle$	10.43	11.28	10.47
$\langle r_1^2\rangle$	26.07	28.21	26.18
Sr $5s5p\ {}^3P_2^o$			
$\langle Q_{zz}\rangle$	6.419	6.080	6.008
$\langle z_1^2\rangle$	5.647	6.400	5.791
$\langle r_1^2\rangle$	23.36	25.28	23.38
Sr $5s4d\ {}^1D_2^e$			
$\langle Q_{zz}\rangle$	4.617		8.749
$\langle z_1^2\rangle$	5.081		5.791
$\langle r_1^2\rangle$	19.86		23.85
Sr $5s5p\ {}^1P_1^o$			
$\langle Q_{zz}\rangle$	2.873		1.366
$\langle z_1^2\rangle$	6.949		7.498
$\langle r_1^2\rangle$	23.72		23.86
Sr $5p5p\ {}^3P_2^e$			
$\langle Q_{zz}\rangle$	−4.744		−4.879
$\langle z_1^2\rangle$	9.488		9.756
$\langle r_1^2\rangle$	23.72		24.39
Ba $6s6p\ {}^3P_2^o$			
$\langle Q_{zz}\rangle$	8.792		8.636
$\langle z_1^2\rangle$	7.216		7.161
$\langle r_1^2\rangle$	30.44		30.12
Ba $6s5d\ {}^1D_2^e$			
$\langle Q_{zz}\rangle$	2.015		9.537
$\langle z_1^2\rangle$	6.658		4.561
$\langle r_1^2\rangle$	21.99		23.22
Ba $6s6p\ {}^1P_1^o$			
$\langle Q_{zz}\rangle$	2.860		0.4626
$\langle z_1^2\rangle$	9.197		9.862
$\langle r_1^2\rangle$	30.45		30.05
Ba $5d5d\ {}^3P_2^e$			
$\langle Q_{zz}\rangle$	−4.136		−4.332
$\langle z_1^2\rangle$	8.272		8.664
$\langle r_1^2\rangle$	20.68		21.66

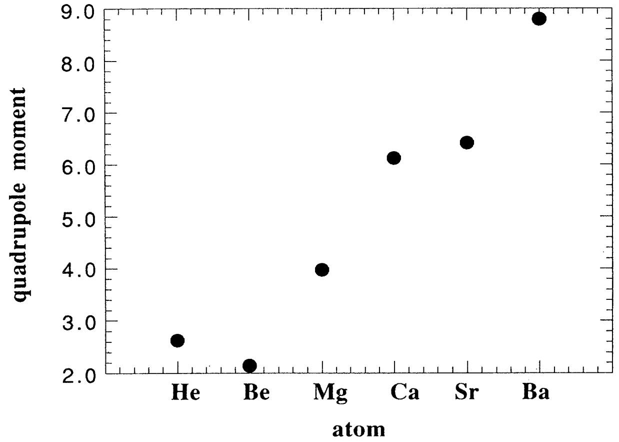

FIG. 1. Quadrupole moments of He** and the alkaline-earth atoms for the *nsnp* $^3P_2^o$ series based on well-converged CI wave functions. Quadrupole moments are in units of ea_0^2.

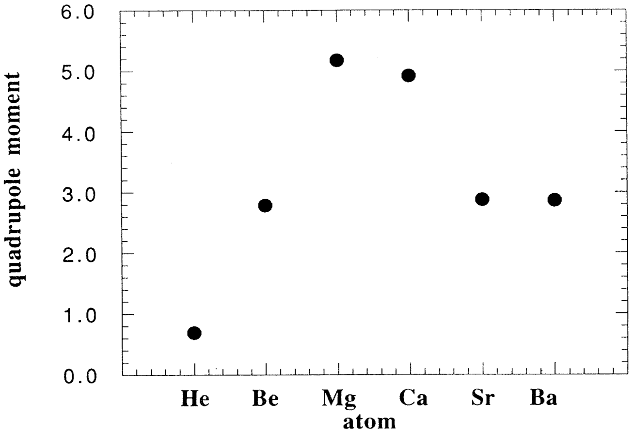

FIG. 3. Quadrupole moments of He** and the alkaline-earth atoms for the *nsnp* $^1P_1^o$ series based on well-converged CI wave functions. Quadrupole moments are in units of ea_0^2.

about the relative validity of the UHF and RV approximate representations of atomic quadrupoles? Statistically, there is not a great deal to favor one approximation over the other. The coefficient of correlation (*R* value) is 0.833 for the RV and 0.918 for the UHF treatments of the alkaline-earth atoms. The corresponding standard errors of the estimates are 2.707 and 2.657, respectively. The UHF approximation is consistently better in representing the quadrupole moments of *D* states than is the RV but the RV tends to do better with the *P* states. Both models represent the $^3P^e$ quadrupoles, the only states with negative values, quite well, but it was previously known that these states are well described by both models. The RV approximation does consistently represent the expectation values of $\langle z_i^2 \rangle$ better than does the UHF for *S* states, but quadrupole moments will not show this of course; some other measure of the spatial distribution of the electron probability density will be required to probe this property. The UHF, except in the case of Be, overestimates the quadrupole moment of the $^1P^o$ resonance levels and the RV underestimates them. On balance, the implication is that the RV model is a better zeroth approximation for the *S* and *P* states but the UHF is better for the *D* states. From this, we might make the tentative supposition that correlation is significantly more important in determining the spatial distribution of the electron probability in *S* and *P* states than in *D* states. However, our sample of *D* states is small, and our comparisons here are with theoretical rather than experimental values. We may hope that some of the predictions based on our CI calculations will soon

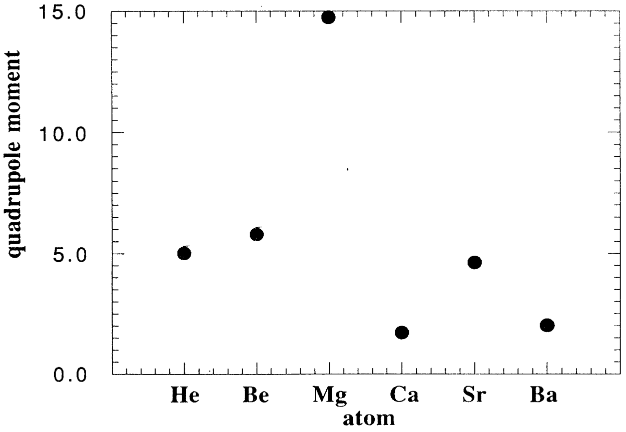

FIG. 2. Quadrupole moments of He** and the alkaline-earth atoms for the *npnp* $^1D_2^e$ series based on well-converged CI wave functions. Quadrupole moments are in units of ea_0^2.

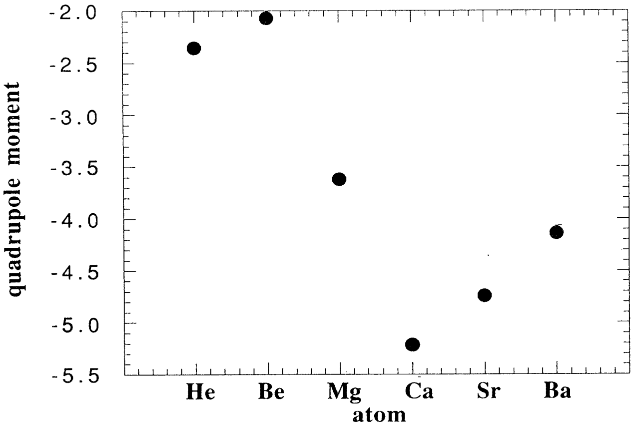

FIG. 4. Quadrupole moments of He** and the alkaline-earth atoms for the *npnp* $^3P_2^e$ series based on well-converged CI wave functions. Quadrupole moments are in units of ea_0^2.

be tested against measured quadrupole moments.

To our knowledge, of all the quadrupole moments given in Table I, the literature contains calculated counterparts for only the ${}^3P_2^o$ and ${}^3P_1^o$ states of beryllium [17]. Sinanoğlu and Beck [17] calculated a quadrupole moment of 2.045 ea_0^2 for the ${}^3P_2^o$ state using non-closed-shell Hartree-Fock or restricted Hartree-Fock (RHF) wave functions. The same authors calculated a quadrupole moment of 2.296 ea_0^2 for the same state with wave functions derived using the non-closed-shell many-electron theory of atoms and molecules (NCMET) of Sinanoğlu. In the latter method, the wave function includes all of the specifically non-closed-shell-type electron correlation effects and is thought to be more accurate than the RHF wave function. As seen in Table I, the CI wave functions yield a quadrupole moment of 2.140 ea_0^2 for the same state which differs from the NCMET quadrupole moment by 7%. The RV wave function yields a quadrupole moment of 1.919 ea_0^2 which differs from the NCMET quadrupole moment by 16%. The quadrupole moments calculated using our pseudopotential-based UHF wave function and using the all-electron RHF wave function of Sinanoğlu and Beck are 1.833 and 2.045 ea_0^2, respectively, which is a difference of 10%. Since we know of no measured values with which to compare any of the quadrupole moments in Table I and since the quadrupole moment is extremely sensitive to the wave function, we take the above statistics as an indication that our calculational procedure is indeed sound.

As discussed earlier, to estimate the accuracy of our results, we have also calculated CI quadrupole moments for two very independent-particle-like, singly excited states of helium since these are, to our knowledge, the only excited two-electron atomic states that have been characterized by *measured* quadrupole moments. These are the He $1s4p$ and $1s5p$ ${}^3P^o$ states. Additionally, we have calculated oscillator strengths for the He $1s2s$ ${}^3S^e \rightarrow 1s4p$ ${}^3P^o$ and He $1s2s$ ${}^3S^e \rightarrow 1s5p$ ${}^3P^o$ transitions. As discussed earlier, our purpose in doing this was to use the oscillator strengths as a test of the wave functions, particularly for the two ${}^3P^o$ singly excited helium states.

The parameters and energies characterizing the relevant wave functions are listed in Table II. The experimental energies are taken from Ref. [28]. In each of these three cases, the difference between the experimental energies and the calculated energies is less than 1 mRY. The CI oscillator strengths for these transitions as well as literature values for these oscillator strengths are given in Table III. The literature values for these oscillator strengths were calculated by Schiff, Pekeris, and Accad [20] using wave functions having up to 364 terms. The authors estimate that their ${}^3S \rightarrow {}^3P$ oscillator strengths are "accurate to within an error of not more than one, or occasionally two, in the last digit quoted." The CI quadrupole moments and measured quadrupole moments for the He $1s4p$ and $1s5p$ ${}^3P^o$ are given in Table IV.

The strong agreement, greater than 99%, between the CI oscillator strengths and the accurately calculated oscillator strengths of Schiff, Pekeris, and Accad [20] seems to indicate that the singly excited helium wave functions are of reliable accuracy. The difference between the experimental and calculated CI quadrupole moments of roughly 14% for the $1s4p$ $4\,{}^3P$ is consistent with the random error reported by Miller and Freund [19]. The larger discrepancy of 38% for the $1s5p$ $5\,{}^3P$ state is well outside their *random error*. However, in their paper on the topic, Miller and Freund warn that a possible source of error might lie in the existence of an electric field, either static or microwave, in the interaction zone. In particular, stray electric fields would make the apparent quadrupole moments too large, which is the direction in which our quadrupole moments differ from theirs [29].

Extensions of the two earlier-mentioned experimental techniques that have been used to measure quadrupole moments of atoms in their ground and excited states may make possible the measurement of many of the quadrupole moments given in Table I. First, Miller and Freund's aforementioned measurement of quadrupole moments of helium using the diamagnetic Zeeman effect is given in Table IV. The transition frequencies between Zeeman levels of $n\,{}^3P$, where $n=4$ or 5, of fine-structure states are induced using microwave radiation and are detected through the resulting change in polarization of the $n\,{}^3P \rightarrow 2\,{}^3S$ fluorescence. $\mathcal{H}'_d$, the effective Hamiltonian for the diamagnetic Zeeman interaction within a given electronic state, can be written in terms of two parts, one that is dependent on the isotropic diamagnetic susceptibility χ_I, and one that is dependent on the anisotropic diamagnetic susceptibility χ_A. The contribution to $\mathcal{H}'_d$ from the anisotropic part gives zero when averaged over all projections whereas the contribution to $\mathcal{H}'_d$ from the isotropic part is independent of the projection of the angular momentum along the magnetic field. The anisotropic diamagnetic susceptibility is related to the quadru-

TABLE II. Energies and parameters characterizing CI wave functions for helium singly excited P states that have measured quadrupole moments and for the He $1s2s$ ${}^3S^e$ state. For these states, one exponent was used for the $l=0$ angular basis functions and another was used for all the others. All energies are given in rydbergs.

State	Number of basis functions	$\xi_{l=0}$	$\xi_{l>0}$	$-E$ (calc.)	$-E$ (expt.)
He $1s4p$ ${}^3P^o$	76	1.47	0.341	$-4.064\,08$	$-4.064\,07$
He $1s5p$ ${}^3P^o$	76	1.47	0.244	$-4.040\,12$	$-4.040\,53$
He $1s2s$ ${}^3S^e$	41	0.880	1.00	$-4.349\,87$	$-4.349\,90$

TABLE III. Oscillator strengths calculated using CI wave functions and those accurately calculated in Ref. [19].

Transition	$f_{ik,\mathrm{CI}}$	$f_{ik,\mathrm{Ref.}[19]}$
He $1s2s\ ^3S^e \rightarrow 1s4p\ ^3P^o$	0.025 78	0.025 77
He $1s2s\ ^3S^e \rightarrow 1s5p\ ^3P^o$	0.012 6	0.012 5

TABLE IV. Quadrupole moments calculated using CI wave functions and those measured in Ref. [18]. All quadrupole moments are given in atomic units of ea_0^2.

State	$Q_{zz,\mathrm{CI}}$	$Q_{zz,\mathrm{Ref.}[18]}$
He $1s4p\ ^3P^o$	-210	-289 ± 45
He $1s5p\ ^3P^o$	-473	-705 ± 45

pole moment as defined by Eq. (1) by

$$\langle L,M_L=L|Q_{zz}|L,M_L=L\rangle \\ =[-8mc^2L(2L-1)]\hbar/e)\chi_A \ , \qquad (19)$$

where χ_A is expressed in Hz/G^2. From Eq. (19) it is obvious that knowledge of χ_A leads directly to Q_{zz}.

The second experimental method that has been used to measure atomic quadrupole moments is atomic beam magnetic resonance. Angel, Sandars, and Pierce used this method to measure the quadrupole moment of the $^2P_{3/2}$ ground state of aluminum in 1967; this was the first experimentally determined atomic quadrupole moment. Later, Sandars and Stewart [30] used the same method to measure the quadrupole moments of the metastable $^3P_2$ states of the rare gases Ne, Ar, Kr, and Xe. In these experiments, an atomic beam apparatus was set to observe a specific Zeeman transition in a magnetic field that was large enough to form the axis of quantization. Under this condition, the energy of a Zeeman sublevel is given by

$$W=g_J\mu_0B-\frac{3M_J^2-J(J+1)}{2J(J-1)}Q_{zz}\frac{\partial E}{\partial z} \\ -\frac{3M_J^2-J(J+1)}{4J(2J-1)}(3E_z^2-E^2)-g_J\mu_0M_J(\mathbf{v}\times\mathbf{E})_z \ . \qquad (20)$$

The first term is the magnetic interaction, with g_J being the g factor and μ_0 the Bohr magneton. The second is the quadrupole interaction containing the quadrupole moment, the third is the quadratic Stark splitting, and the fourth is the interaction between the magnetic moment of the atom and the magnetic field it experiences as it moves with velocity **v** through the electric field **E**.

The basic difficulty in the experiment is that the quadrupole interaction must be separated from the larger quadratic Stark effect and the $\mathbf{v}\times\mathbf{E}$ effect. The quadrupole interaction can be distinguished from the quadratic Stark effect because, upon reversing the direction of the electric field, the sign of the quadrupole interaction changes but that of the quadratic Stark term remains unchanged. The quadrupole term can be distinguished from the $\mathbf{v}\times\mathbf{E}$ term by reversing the direction of the magnetic field which changes the sign of the $\mathbf{v}\times\mathbf{E}$ term but leaves the quadrupole interaction term unchanged.

Whatever the physical methods used, the point is clear: it is now possible to learn a great deal about atoms by measuring or calculating for them a physical constant characteristic of molecules and nucleii.

ACKNOWLEDGMENTS

This research was supported by a grant from the National Science Foundation. S.C.C. would like to thank John Hunter III for helpful discussions and for reading the manuscript.

[1] R. P. Madden and K. Codling, Phys. Rev. Lett. **10**, 516 (1963).

[2] J. W. Cooper, U. Fano, and F. Prats, Phys. Rev. Lett. **10**, 518 (1963).

[3] C. D. Lin, Phys. Rev. A **29**, 1019 (1984); U. Fano, Rep. Prog. Phys. **46**, 97 (1983); C. D. Lin, Adv. At. Mol. Phys. **22**, 77 (1986).

[4] M. E. Kellman and D. R. Herrick, Phys. Rev. A **22**, 1536 (1980).

[5] D. R. Herrick, M. E. Kellman, and R. D. Poliak, Phys. Rev. A **22** 1517 (1980).

[6] R. S. Berry, in *The Lesson of Quantum Theory,* edited by J. deBoer and O. Ulfbeck (North-Holland, Amsterdam, 1986).

[7] R. S. Berry and J. Krause, Adv. Chem. Phys. **70** (1), 35 (1988).

[8] G. S. Ezra and R. S. Berry, Phys. Rev. A **28**, 1974 (1983).

[9] G. S. Ezra and R. S. Berry, Phys. Rev. A **25**, 1513 (1982).

[10] G. S. Ezra and R. S. Berry, Phys. Rev. A **28**, 1989 (1983).

[11] J. L. Krause and R. S. Berry, Phys. Rev. A **31**, 3502 (1985).

[12] J. L. Krause and R. S. Berry, J. Chem. Phys. **83**, 5153 (1985).

[13] J.L. Krause and R. S. Berry, Comments At. Mol. Phys. **18**, 91 (1986).

[14] J. E. Hunter III and R. S. Berry, Phys. Rev. A **36**, 3042 (1987).

[15] J. E. Hunter III and R. S. Berry, Phys. Rev. Lett. **59**, 2959 (1987).

[16] A. deShalit and H. Feshbach, *Theoretical Nuclear Physics* (Wiley, New York, 1974); Chaps. 1 and 6.

[17] O. Sinanoğlu and D. R. Beck, Chem. Phys. Lett. **21**, 247 (1973).

[18] T. A. Miller and R. S. Freund, Phys. Rev. A **4**,81 (1971).

[19] T. A. Miller and R. S. Freund, Phys. Rev. A **5**, 5188 (1972).

[20] B.Schiff, C. L. Pekeris, and Y. Accad, Phys. Rev. A **4**, 885 (1971).

[21] A. D. Buckingham and R. L. Disch, Proc. R. Soc. **273**, 275 (1963).

[22] J. R. P. Angel, P. G. H. Sandars, and G. K. Woodgate, J. Chem. Phys. **47**, 1552 (1967).

[23] G. B. Bachelet, D.R. Hamann, and M. Schlüter, Phys. Rev. B **26**, 4199 (1982).
[24] J. Batka and R. S. Berry (unpublished).
[25] D. M. Brink and G. R. Satchler, *Angular Momentum* (Clarendon, Oxford, 1968).
[26] I.S. Gradshteyn and I. M. Ryzhik, *Table of Integrals, Series, and Products* (Academic, New York, 1965).
[27] R. N. Zare, *Angular Momentum: Understanding Spatial Aspects in Chemistry and Physics* (Wiley, New York, 1988).
[28] C. E. Moore, *Atomic Energy Levels as Derived from Analyses of Optical Spectra,* Natl. Bur. Stand. (U.S.) Circ. No. 467 (U.S. GPO, Washington, DC, 1949); Vol. I.
[29] R. S. Freund (private communication).
[30] P. G. H. Sandars and A. J. Stewart, Phys. **3**, 429 (1973).